The Journal of CPRI,
Vol. 4, No. 2, September 2008 pp. 185–194

Electroluminescence and Space Charge in Nanodielectrics subjected to AC Voltage

S S Bamji*, M Abou-Dakka*, A Bulinski* and L Utracki*

Electroluminescence (EL) and Phase Resolved Pulsed Electro-Acoustic (PRPEA) techniques are used to determine charge injection and space charge distribution in insulation subjected to an AC electric field. It is shown that both EL and PRPEA can provide information about the dynamics of charge injection and trapping in solid dielectrics under an AC field. Such techniques are useful in evaluating novel materials, such as nanodielectrics, for use in power apparatus.

1.0 INTRODUCTION

Polymeric materials are extensively used in power apparatus such as high voltage cables, transformers and capacitors. They have excellent electrical properties such as high breakdown strength, low dielectric losses, and high DC resistance. In addition, good mechanical properties, high corrosion resistance, ease of processing, low cost of maintenance and environmental concerns often makes them a better choice over the oil-based systems.

There is a considerable demand for compact, eco-friendly, highly reliable and more efficient high voltage devices. This can be achieved by developing novel insulating materials such as nanodielectrics, i.e. dielectric materials containing nano-particles, which could withstand higher electrical and mechanical stresses, higher temperatures, etc. However, the formation of space charge in these materials can cause field distortions and give rise to dissipative energetic processes which affect the onset of electrical ageing, decrease the withstand voltage and lead to insulation failure [1]. The determination of space charge injection and distribution in the polymer is not only helpful for developing new insulating materials but also for improving the design of existing high voltage apparatus based on traditional insulating systems.

Electroluminescence (EL), the emission of light in dielectrics subjected to high electric stress, has been successfully applied to detect charge injection and the very early stages of degradation of insulation used in high voltage devices [2]. The injected charge accumulates in the material as a space charge, which plays a major role in DC voltage applications and cannot be completely ignored in AC applications.

Isotactic polypropylene (PP) is extensively used in power capacitors and other high voltage devices. This paper describes the dielectric properties of PP with and without nanoparticles. The electroluminescence technique is employed to detect light emission and show its relevance to charge injection and space charge accumulation in polymeric insulation. The Pulsed Electro-Acoustic (PEA) technique is routinely employed to measure space charge distribution in polymeric insulation subjected to a DC field [3]. In the present work, the newly

*National Research Council, Canada, Ottawa, Ontario, Canada, K1A 0R6

developed Phase Resolved Pulsed Electro-Acoustic (PRPEA) technique [4] is used to determine the space charge distribution in insulation subjected to an AC electric field. It is shown that both EL and PRPEA provide information about the dynamics of charge injection and trapping in solid dielectrics under an AC field and are useful in evaluating new materials, such as nanodielectrics, for use in power apparatus.

2.0 EXPERIMENTAL INVESTIGATION

2.1 Sample preparation

Three materials, isotactic PP with 0, 2, and 4-wt% of organosilicate, referred to in this text as PP-0%, PP-2%, and PP-4%, respectively, were used. The manufacture of polypropylene containing nanoparticles involved two steps:

1. Preparation of the Master Batch (MB)

PP (ProFax PDC 1274 from Basell) was melt compounded with a 1:1 mixture of two compatibilisers [PP grafted with maleic anhydride (PP-MA) from Eastman (Epolene-3015) and from Crompton (Polybond 3150)] and organoclay (Cloisite 15A, C15A, from SCP, i.e., montmorillonite pre-intercalated with excess of di-methyl di-hydrogenated tallow ammonium chloride). The compounding at 200°C was carried out under a blanket of dry nitrogen in a twin-screw extruder (TSE) with a gear pump and an extensional flow mixer (EFM) having a gap of 63.5 μm. The TSE throughput was Q = 10kg/h. For comparison, the same compounding conditions were applied using the TSE alone. The resulting MB composition was: 88-wt%PP + 8-wt%PP-MA + 4-wt%C15A. The organoclay dispersion of PP-4% was characterised by X-ray diffraction (XRD) and high-resolution transmission electron microscopy (HRTEM). The interlayer spacing was d_{001} = 3.25 nm; the number of clay platelets in residual stacks N = 3.25, and the degree of exfoliation EX = 79%, i.e., 11% above that observed for extrusion using TSE alone.

2. Preparation of the test samples

To ascertain the same compounding history of the three samples tested, PP-0%, PP-2% and PP-4% were extruded at 180°C under a blanket of dry nitrogen, using a single screw extruder (SSE) and EFM with a 15 μm gap. The throughput was Q = 10 kg/h. Thus the MB obtained in Step 1 was re-extruded in the SSE+EFM compounding line, followed by dry-blend of PP with MB at a ratio 1:1, and neat PP. The composition of PP-2% was: 92-wt%PP + 4-wt%PP-MA + 2-wt%C15A. The clay dispersion parameters were: d_{001} = 3.45 nm, N = 2.64, and EX = 88%, i.e., 20% above that from TSE.

The three materials were moulded using a hot press at 210°C under a pressure of 50 MPa to produce flat sheets with a thickness of 135 ± 5 μm. Each side of the sample was sputtered with gold electrodes having a diameter and thickness of 25 mm and 30 nm, respectively. Space charge distribution or EL was measured when each sample was individually subjected to an AC field inside the respective test-cell.

Breakdown (BD) Tests: The AC and DC breakdown tests were performed according to ANSI/ASTM D 149-75 and D 3755-79 standard methods, respectively. To minimise the effect of partial discharges, the tests were performed in silicon oil. For DC and AC tests, the voltage was increased at a rate of 90 V/s and 70 V/s, respectively, till breakdown. A PC controlled TREK 20/20 high voltage amplifier provided stable and repeatable voltage increase rates. RMS values of AC breakdown voltage and field are reported throughout this paper.

2.2 Electroluminescence under a uniform AC electric field

To detect EL under a uniform AC field the sample was placed in a light-tight holder, shown in Fig. 1. To prevent any spurious light from entering the detector, EL emitted from only the central region of the sample was monitored. The

sample holder was placed inside a light-tight chamber, shown in Fig. 2, which was pressurised to 125 kPa with ultra-high purity nitrogen to avoid partial discharges (PD).

A sinusoidal waveform having 57,000 digital data points was fed to an arbitrary waveform function generator. The output from this generator was amplified by a Trek 20/20 high voltage amplifier and applied to the high voltage electrode of the sample. The AC field was increased from 0 to 36 kV/mm in steps of 2 kV/mm with 180 s at each step. The EL emitted from the sample was measured at each step of the applied field.

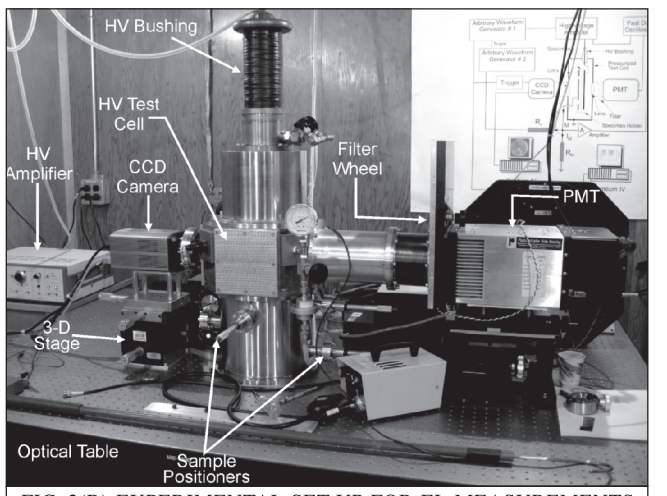

FIG. 2(B) EXPERIMENTAL SET-UP FOR EL MEASUREMENTS UNDER UNIFORM FIELDS

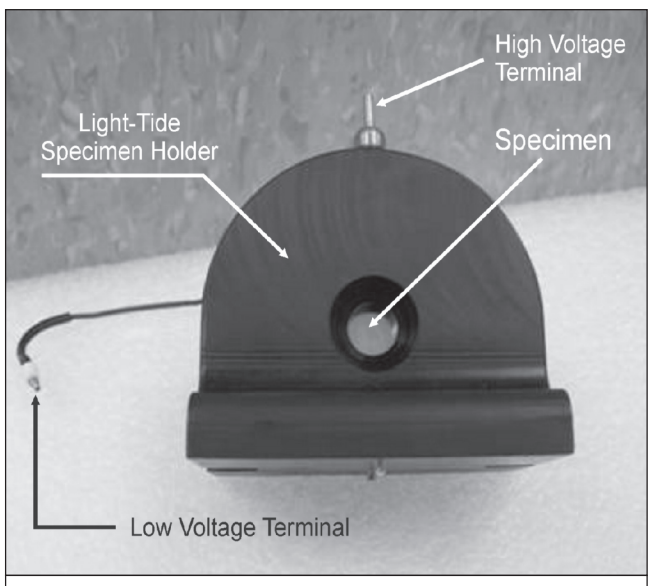

FIG. 1 SAMPLE HOLDER FOR EL MEASUREMENTS

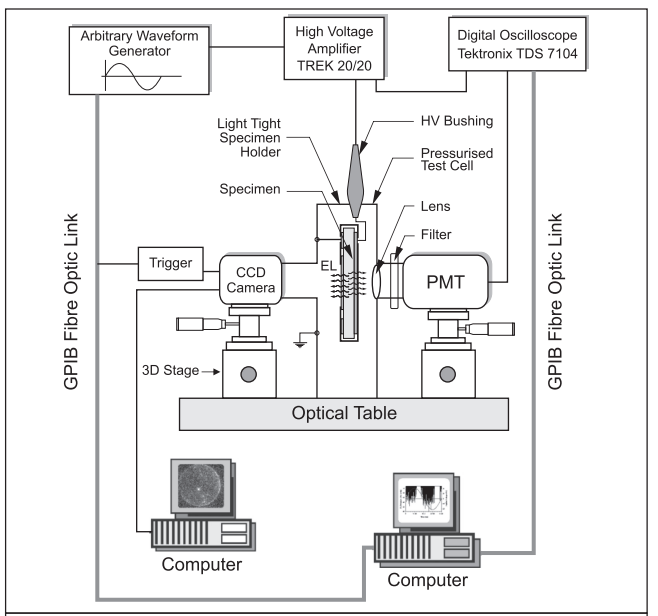

FIG. 2 (A) BLOCK DIAGRAM

EL was captured by a photomultiplier tube operating in the pulse counting mode. The tube was cooled to –30°C to minimise the dark pulse counts. Spurious light that could be emitted due to the roughness (of the order of a few nanometers) at the gold-polymer contact was removed by using a band-pass filter that cut off any transmission above 600 nm. The EL pulses were recorded with a Tektronix TDS 7404 scope (4 GHz, 20 GS/s) and the data were then transferred to a computer for analysis. A CCD camera captured the image of the EL emitting region which was transferred to another computer. The entire system was automated to simultaneously obtain the spectral and spatial resolution of EL emitted in the specimen.

Phase Resolved PEA technique: To measure space charge distribution at various phase angles of the AC waveform, a commercially available PEA system was modified, as shown in Fig. 3. AC voltage at 50 Hz from Function Generator 1 was amplified with a high voltage amplifier and then applied to the specimen held in the PEA test cell. Function Generator 2, synchronised to ≤1 ns with Function Generator 1, triggered a fast pulse generator to produce narrow electrical pulses (5 ns, 400 V) at any phase angle, between 0° to 360°, of the voltage waveform. The pulses were precisely synchronised to the applied voltage by dedicated software developed for this purpose and only one pulse was applied during each voltage cycle.

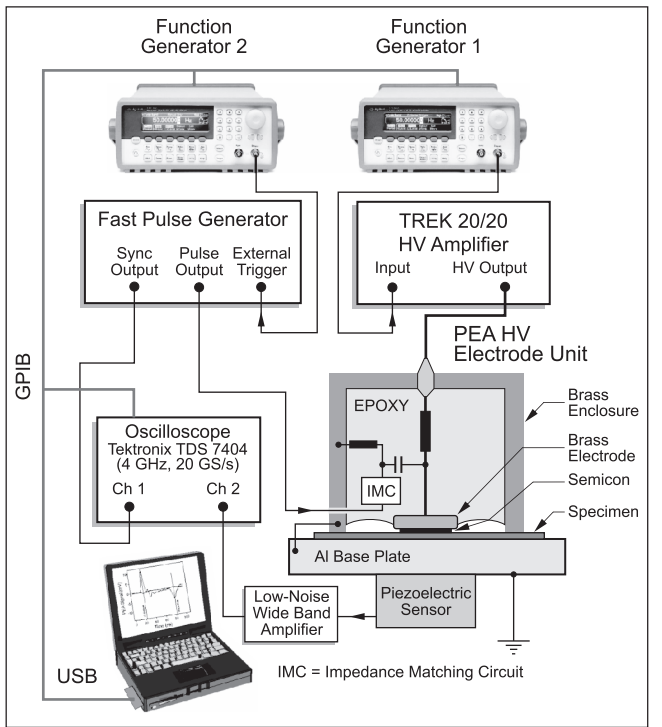

FIG. 3 BLOCK DIAGRAM OF THE PHASE RESOLVED PEA SETUP

The narrow electrical pulses acting on the space charge in the insulation create pressure waves that travel through the specimen and are detected by a piezoelectric sensor attached to the low-voltage electrode. The response of the piezoelectric transducer is captured by a fast digital scope (Fig. 3), operating at 20 GS/s and having a bandwidth of 4 GHz. Since the low-voltage electrode represents a delay line for the pressure wave, a delay of 1.55 μs was required to trigger the scope. The sensitivity of the system was enhanced by decreasing the sampling time to 40 ps/point. The signal to noise ratio was improved by averaging the output signal over several hundred cycles of the AC waveform. A constant pressure was applied to the specimen and a laptop controlled all the instruments and automated the measurements [4].

Each specimen was electrically stressed with an AC field which was increased, in steps of 2 kV/mm, from 0 to 20 kV/mm. The narrow pulses were initially applied at 0° phase angle of the AC waveform and the computer then automatically increased the phase angle, in steps of 15°, till 360°. The data at each step of the applied field were acquired for 20 min.

3.0 RESULTS AND DISCUSSION

EL emission in PP

The spatial resolution of EL emitted in PP subjected to a uniform field at 36 kV/mm and captured by the CCD camera (Fig. 2) is shown in Fig. 4. Although the intensity of light across each sample was quite uniform, it had a few bright spots.

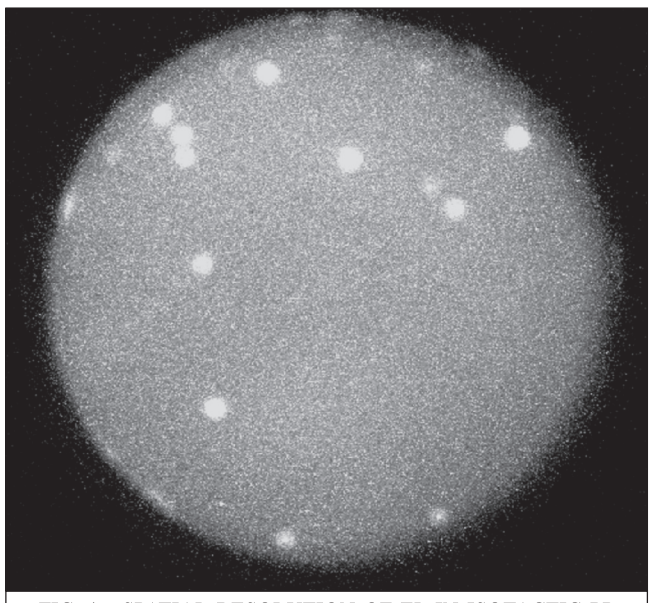

FIG. 4 SPATIAL RESOLUTION OF EL IN ISOTACTIC PP

These bright spots could be due to surface plasmons [5], which are the oscillation of the electron gas in the thin gold electrode at the surface of the insulation. Usually, surface plasmons do not emit light but when they interact with some irregularities of the order of a few nanometers, such as at the gold-polymer interface, they start emitting in the 650 to 800 nm range, with a peak at 750 nm. To remove the light caused by surface plasmons, a band-pass filter with a cut-off at wavelengths above 600 nm was used.

Fig. 5 shows the number of EL pulses emitted from samples of isotactic PP as a function of the applied field. The graph shows that EL emission does not occur at low electric fields but starts at ~ 18 kV/mm and then its intensity increases non-linearly with the applied field.

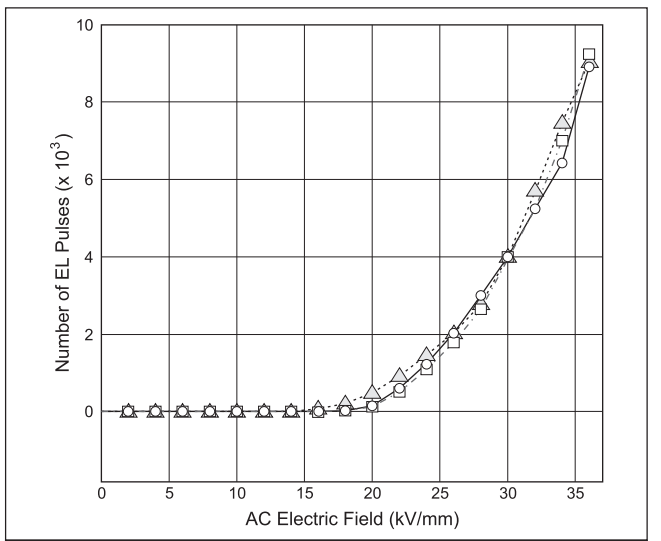

FIG. 5 EL IN ISOTACTIC PP VERSUS THE APPLIED AC FIELD

A possible mechanism as to how and why light can be emitted when AC high voltage is applied to the polymer is shown in Fig. 6. A polymeric insulation can be represented by the band-gap model where E_c stands for the conduction band and E_v stands for the valence band. An insulator such as PP has a wide band but due to imperfections, additives etc., there are many trapping states in the band gap. Antioxidants and the complex product mixtures that are formed by reactions with oxygen during the moulding of the polymer provide non-volatile species which act as trapping centers [6]. These species also act as recombination centers for charges of both polarities. The various trapping states can be represented as shallow and deep traps just below the conduction band for electrons and shallow and deep traps just above the valence band for holes.

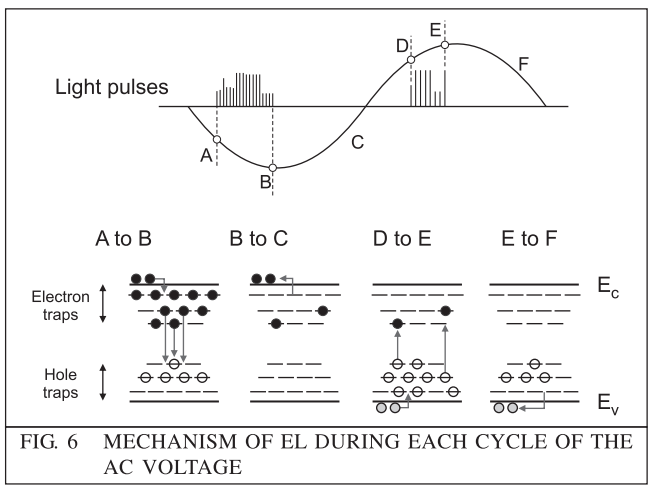

FIG. 6 MECHANISM OF EL DURING EACH CYCLE OF THE AC VOLTAGE

When an AC waveform is applied to the sample during the negative half cycle, at a certain threshold voltage denoted by A, electrons get injected into the polymer. These electrons become trapped in the shallow and deep traps of the polymer. Some of the electrons trapped in deep traps recombine with the holes, which were injected into the polymer during the previous positive half cycle and which could not detrap when the polarity was reversed. The recombination of the electrons and the holes gives rise to light emission.

During the portion B to C of the negative half cycle, the electrons in the shallow traps detrap but those in the deep traps cannot. When the polarity reverses, above a certain threshold voltage denoted by D, holes are injected into the polymer and are trapped in the shallow and deep traps of the polymer. Some of these holes will recombine with the electrons in the deep electron traps of the polymer and light is again emitted.

When the voltage decreases from E to F, the holes in the shallow traps will detrap but those in the deep traps cannot, so they remain in the insulation. Some of these trapped holes will recombine with the electrons emitted during the next negative half-cycle to give rise to EL. This process is repeated every cycle of the AC voltage and since the light is caused by the application of high electric field, the phenomenon of light emission is called electroluminescence.

Phase Resolved PEA (PRPEA) technique: The PEA signal from the PP film, obtained as a function of time, when the narrow electrical pulses are applied at various phase angles of an AC electric field at 20 kV/mm is shown in Fig. 7. These are the signals from the transducer that were captured and averaged by the scope over 300 voltage cycles.

The deconvolution of a PEA signal using Fast Fourier Transform (FFT) gives the profiles of the space charge density and electric field distributions in the insulation.

During measurements with the DC field, the high DC voltage is prevented from entering the fast pulse generator by a coupling capacitor [7]. In addition, a high voltage resistor and an impedance matching circuit are all embedded in the PEA high voltage electrode (Fig. 3). Under an AC field, these components would cause a certain phase shift between the input and the output voltage of the high voltage amplifier which would depend on the frequency of the applied voltage. It is important to know this phase shift in order to determine when to trigger the application of fast pulses to the specimen so that they would precisely align with the pre-determined phase angle of the AC voltage applied to the insulation.

In the previous work [8], the application of fast pulses was correlated with a phase angle of the output voltage from Function Generator No. 1 (Fig. 3) rather than, as done in the current work, with the output voltage of the high voltage amplifier, i.e., the voltage applied to the specimen. In Fig. 7, the output signals from the piezoelectric sensor were corrected for the phase shift described above.

The narrow electrical pulses were initially applied at 0° phase angle of the applied voltage and then in 15° increments till 360°. When an electric field is applied to PP film held between two electrodes, image charges are induced at each electrode. The magnitude of the image charge depends on the applied electric field and the distribution of the space charge density in the film. Fig. 7 shows that the PEA signals at all phase angles display peaks at the electrodes.

At the phase angle of 0°, small negative and positive peaks appear at the low and high voltage electrodes, respectively. The peak at the low voltage decreased with further increase of the phase angle until it reached a minimum at 90°. Above 90°, the peak increased, again reversed polarity at a phase angle of 180° and reached a maximum at 270°. The peak then started to decrease and at 360°, it had a value close to that at 0°.

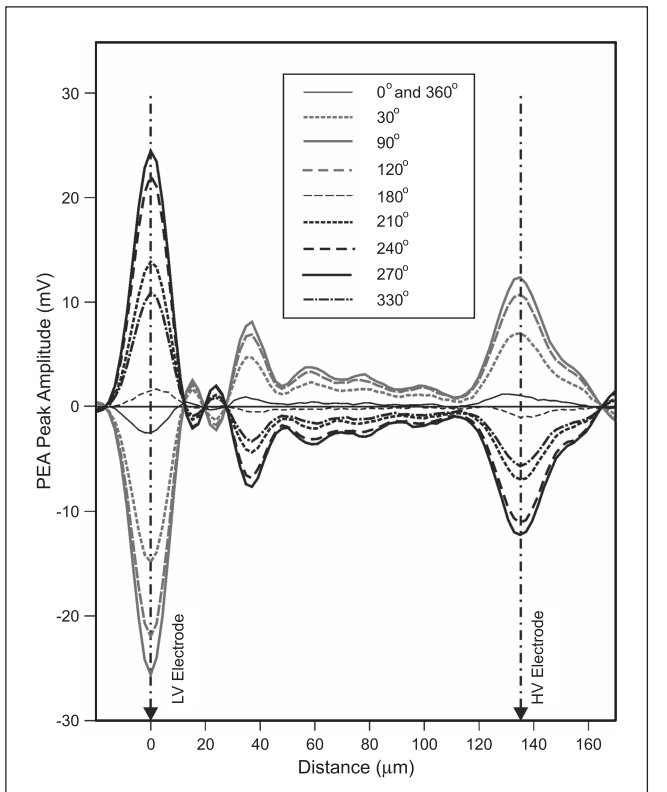

FIG. 7 PEA SIGNAL AS RECORDED BY AN OSCILLOSCOPE FOR PP SUBJECTED TO AN AC FIELD OF 20 kV/mm

A similar trend was observed for the peak at the high voltage electrode, except that its polarity was opposite to that at the low voltage electrode. This is shown in detail in Fig. 8.

Due to the attenuation and scattering of the pressure waves as they traverse the insulation, the peaks at the high voltage electrode decrease

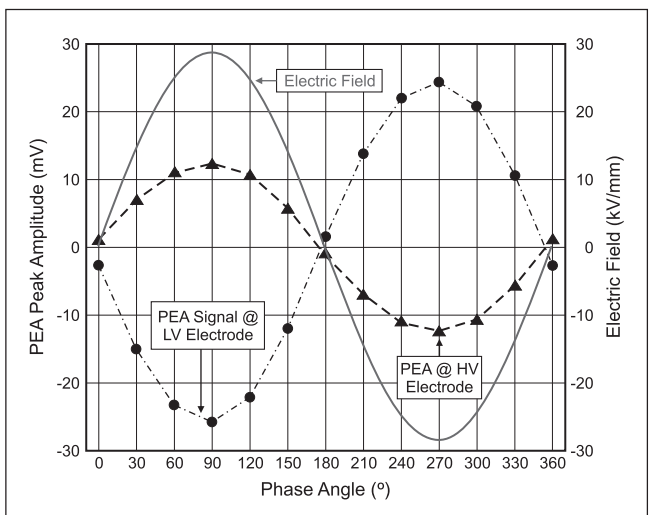

FIG. 8 EFFECT OF PHASE ANGLE OF THE APPLIED AC FIELD ON PEA PEAKS

in magnitude and broaden in width. The change in the polarity of the PEA peaks at both electrodes occurring at certain phase angles of the applied field is consistent with the bipolar nature of charge injection and follows the dynamics of the charge injected into the insulation under an AC field.

Fig. 9 shows the amplitude of the PEA signal peaks at the low voltage electrode versus the applied electric field for a phase angle of 120°. At low electric fields, there is a linear relationship between the peak amplitude of the PEA signal and the applied field. However, above 18 kV/mm a deviation from linearity occurs and increases with field intensity.

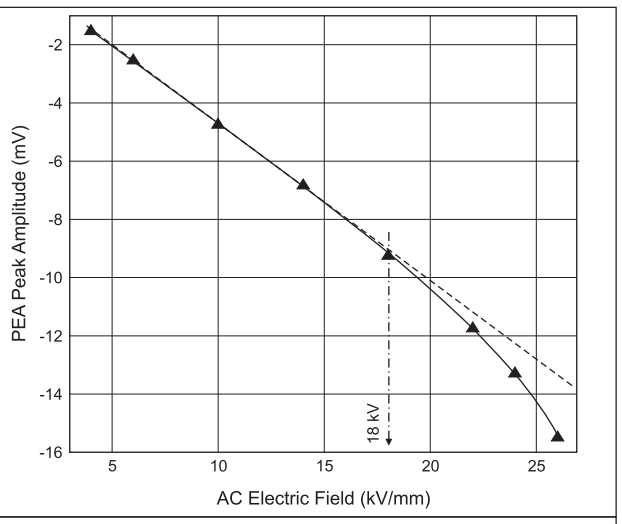

FIG. 9 PEAK AMPLITUDE OF THE PEA SIGNAL AT THE LOW VOLTAGE ELECTRODE VERSUS THE APPLIED AC FIELD FOR A PHASE ANGLE OF 120°

The deviation from linearity is caused by the space charge, which modifies the local stress near the electrodes. Similar results have been reported with the Laser Induced Pressure Pulse (LIPP) method [9], but during the LIPP measurements several factors, such as power variation between consecutive laser shots, target efficiency and target ablation, could have caused certain variations in the magnitude of the measured signals.

Comparison of Figs. 5 and 9 shows a good correlation between the initiation field of EL emission and the field at which the amplitude of the PEA signal at the low voltage electrode starts deviating from linearity.

Thus, without any rigorous mathematical treatment, simple processing of the results obtained by the PRPEA technique can quite accurately determine the electric field at which charges are injected into the insulation.

3.1 PP containing nanoparticles

The DC and AC breakdown strength of the three materials, PP-0%, PP-2%, and PP-4%, are shown in Fig. 10. The error bars in this figure indicate 95% confidence intervals of the Weibull distribution. The graph shows the average value of a minimum of ten breakdowns for each material. Adding organoclay to PP increases the DC breakdown strength.

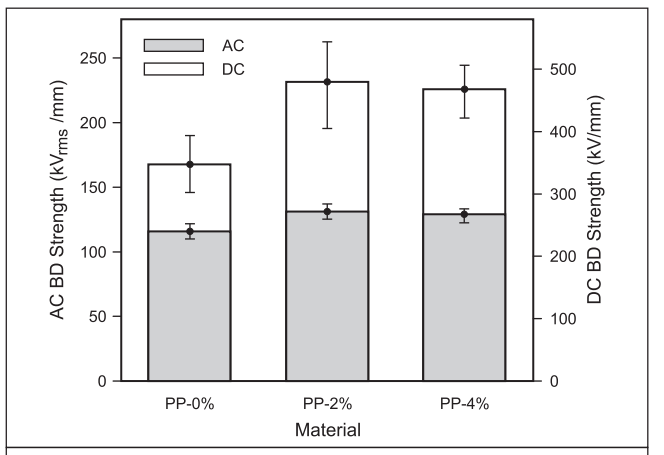

FIG. 10 AC AND DC BREAKDOWN VALUES OF PP WITH AND WITHOUT NANOPARTICLES

Charges could be trapped at the nanofiller-polymer matrix interfaces and thus decrease the probability of breakdown. For the three materials tested in this work, PP-2% had the highest breakdown strength, as shown in Fig. 10. The slightly lower AC and DC BD strength of PP-4%, as compared to PP-2%, could be due to the decrease in spherulite size and density and poorer dispersion of the nanoparticles.

Fig. 11 shows typical EL emissions from the three materials subjected to AC fields. At least five samples of each material were tested. Adding organoclay to PP does not increase the EL inception field (~18 kV/mm) but, compared to PP-0%, the EL intensity was usually lower in PP-2% and higher in PP-4%. At low electric fields, EL

emission in polyolefin is caused by the recombination of electrons and holes injected into the insulating material subjected to an AC voltage. Enone and poly-(enone) sequences have been identified as luminescent centers in PP [6]. These polar species have equal affinity for electrons and holes and act as recombination centers for charges of both polarities injected into the material.

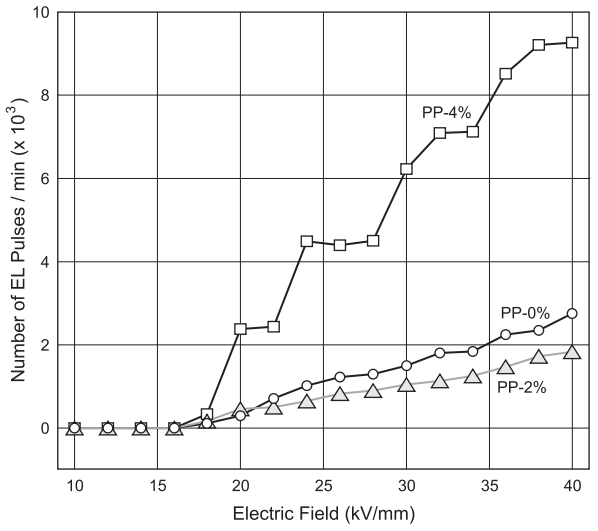

FIG. 11 EL EMISSION IN PP WITH THREE DIFFERENT CONCENTRATIONS OF NANOPARTICLES VERSUS THE APPLIED AC FIELD

In the nanocomposites, the nanoparticles could provide additional recombination centers and this would increase the intensity of EL emission as in PP-4%. However, the EL intensity of PP-2% was less than PP-0% and this suggests that less charge is injected into PP-2% as compared to the other two materials. Resolving the space charge distribution in the material with the PRPEA technique (described below) further substantiates this hypothesis.

Fig. 12 shows the space charge distribution obtained by the PRPEA technique in PP, containing 0%, 2%, and 4% by weight of nanoparticles, when subjected to AC fields of 2 kV/mm, 20 kV/mm and 30 kV/mm. No space charge was detected at 2 kV/mm, but at 20 kV/mm, two peaks (one positive at 22 μm and one negative at 34 μm) from the low voltage electrode appeared in all three materials. PP-2% had less space charge than the other two materials and even at the maximum electric stress of 30 kV/mm, it had the smallest peak at 22 μm and 34 μm. This experimental evidence that PP-2% has less space charge than PP-0% and PP-4% may explain why PP-2% has the lowest EL intensity. Evidently, less charge is injected into PP-2%. The double-layer formed across the metal-polymer interface governs the charge transfer from the metal into the insulation and could be influenced by the contamination at the surface of the material.

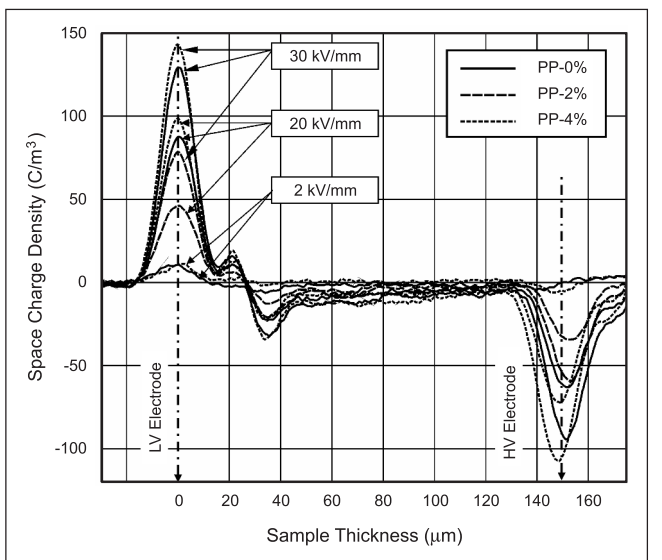

FIG. 12 SPACE CHARGE DISTRIBUTION IN PP-0%, PP-2% AND PP-4% CHARGED AT AC FIELDS OF 2 kV/mm, 20 kV/mm AND 30 kV/mm

4.0 CONCLUSIONS

EL and PRPEA techniques complement each other for determining charge injection and the distribution of the space charge in polymeric insulation subjected to AC electric fields. It is shown that at low electric fields the maximum amplitude of the PRPEA signal changes linearly with the applied voltage. However, above a certain threshold, which coincides with the EL inception field, there is a deviation from linearity. Both EL and PRPEA can provide information about the dynamics of charge injection and trapping in solid dielectrics under AC fields.

EL and PRPEA have been successfully employed to characterise PP films containing nano-particles. Polypropylene containing only 2% by

weight of organo-silicate (PP-2%) had less space charge than PP-0% and PP-4% and this may explain why PP-2% had the lowest EL intensity.

5.0 ACKNOWLEDGMENTS

The authors would like to acknowledge the technical assistance of their colleagues from NRC Canada: Chen Y, McIntyre D and Simard Y.

REFERENCES

[1] Dissado LA and Fothergill J C, Electrical Degradation and Breakdown in Polymers, London, UK, Peter Peregrinus, 1992.

[2] Tohyama K, Bamji S S and Bulinski A T, "Simultaneous Measurement of EL and Dissipation Current in Cable Insulation", Proc. 2003 Intl. Conf. on Properties and Applications of Dielectric Materials (ICPADM'2003), Nagoya, Japan, June 21–26, pp. 1051–1054, 2003.

[3] Fukunaga K, "Innovative PEA Space Charge Measurement Systems for Industrial Applications", IEEE Electrical Insulation Magazine, Vol. 22, No. 2, pp. 18–26, 2004.

[4] Bamji S, Abou Dakka M, and Bulinski A, "Phase-Resolved Pulsed Electro-Acoustic Technique to Detect Space Charge in Solid Dielectrics Subjected to AC Voltage", IEEE Trans. Dielectrics and Electrical Insulation, Vol. 14, No. 1, pp. 77–82, 2007.

[5] Raether H, Surface Plasmons, Berlin, Springer Verlag, 1980.

[6] Tesyssedre G, Laurent C, Montanari G C, Campus A and Nilsson U H, "From LDPE to XLPE: Investigating the Change of Electrical Properties, Part II: Luminescence", IEEE Trans. Dielectrics and Electrical Insulation, Vol. 12, No. 3, pp. 447–454, 2005.

[7] Maeno T and Fukunaga K, "High-Resolution PEA Charge Distribution Measurement System", IEEE Trans. Dielectrics and Electrical Insulation, Vol. 3, No. 6, pp. 754–757, 1996.

[8] Bamji S S and Bulinski A T, "Electro-luminescence and Space Charge Distribution in Polymeric Insulation Subjected to AC Voltage", Proc. 2007 Intl. Conf. on Polymeric Materials in Power Engineering (ICPMPE'2007), Bengaluru, India, Paper III A-2, October 4–6, 2007.

[9] Ho Y F F, Chen G, Davies A E, Swingler S G, Sutton S J, Hampton R Nand Hobdell S, "Measurement of Space Charge in XLPE Insulation under 50 Hz AC Electric Stress Using LIPP Method", IEEE Trans. Dielectrics and Electrical Insulation, Vol. 9, No. 3, pp. 362–370, 2002.

Readers are invited to offer their comments on the article. Please fill in the Reader's Forum.